

Fig. S1. A) Comparison of relative sinking velocity for species reported in Caromel et al (2014), Takahashi & Bé (1984) and Fok-Pun and Komar (1983) that are also present in this study. Open grey points are those published in the literature whilst black points are velocities determined here. B) Comparison of sinking velocities between all species reported in Caromel et al, 2014 (Caromel), Takahashi & Bé, 1984 (Takahashi) and Fok-Pun and Komar, 1983 (Fok-Pun) and the data from this study (Walker). Each point represents an individual foraminifera (or model).

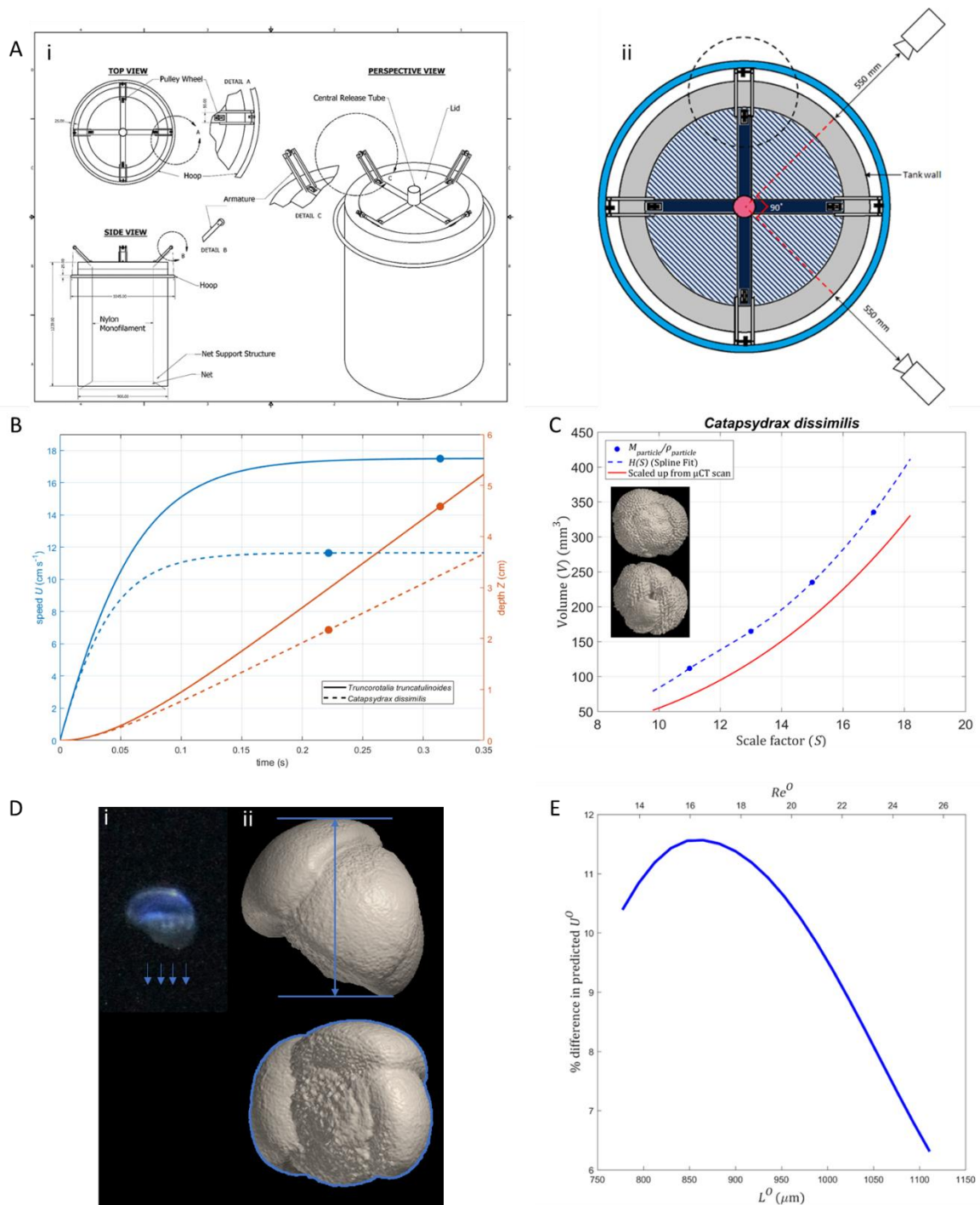


Fig. S2. Settling Tank, theoretical settling velocities, 3D printer limitations, measuring particle characteristics and empirical and theoretical confirmation.

- A i) Schematic of the tank and model retrieval system. All measurements in mm.
- A ii) the tank and camera positions. An external hoop (light blue) was used to raise the net from the bottom of the tank, via the system of pulleys and nylon monofilament mounted on the armatures (one circled with black dashed line). The support arms (dark blue) held a central tube (pink) where the release mechanism was mounted. A ledge (grey) around the top of the tank was used to support the

armatures, support arms and cover for when the tank was not in use. The open part of the tank is shown with dark blue hatching.

- B. Theoretical unsteady solution for speed and depth of spheres released from rest in the experimental tank, with parameters chosen to approximate those of actual models of *T. truncatulinoides* and *C. dissimilis*. Circles represent values when terminal velocities are effectively reached, defined as $0.999 U(t = \infty)$.
- C. Differences in measured (via mass balance, blue) and expected (scaled up from digital surface mesh, red) model volumes versus scale factor for *C. dissimilis*. Inset: Scanned *C. dissimilis* specimen from a spiral (top) and aperture (bottom) view; maximum length is 610 μm .
- D.
 - D i) An example high resolution image of a sinking foraminifera model (*Globoconella inflata*).
 - D ii) Top: The computer-generated model of the same specimen rotated to the sinking orientation, with the maximum length parallel to the flow (L). Bottom: underside view of the foraminifera, i.e. the projected area perpendicular to the flow as the foraminifera sinks, with the projected area (A) outlined in blue.
- E. Relative difference between predicted U^0 based on our empirical $C_D^E(Re)$ curve versus the theoretical $C_D^M(Re)$ curve for hypothetical hollow spherical particles in seawater. Re^0 is based on operating point prediction using $C_D^M(Re)$.

Table S1. Examples of how one might implement our method to study settling of other biological particles. Typical particle sizes and densities are given, followed by estimates of Re^0 and C_D^0 assuming filamentous diatom chains (with the theoretical $C_D(Re)$ relationship for cylinders at low Re , (Batchelor, 1959, Eq 4.10.16, p. 246)), and spherical particles for all other examples. If the proposed working fluids were used with 3D printed models similar to those used in our study ($\rho_{particle} = 1120 \text{ kg m}^{-3}$), one would require models of the listed approximate scales and sizes, which would be expected to sink at the listed speeds. For reference, for air $\rho_{fluid} = 1.225 \text{ kg m}^{-3}$ and $\mu = 1.85 \times 10^{-5} \text{ Pa s}$, and for water $\rho_{fluid} = 1000 \text{ kg m}^{-3}$ and $\mu = 0.001 \text{ Pa s}$ (Munson et al., 1994). It should be noted that water could be used to study particles that normally operate in air, and that the density of the fluid needs to be lower than the density of the model in order for the model to sink. Alternative fluids include low viscosity silicone oils ($\rho_{fluid} = 918 \text{ kg m}^{-3}$, $\mu = 0.004 \text{ Pa s}$), glycerol/glycerine ($\rho_{fluid} = 1260 \text{ kg m}^{-3}$, $\mu = 0.943 \text{ Pa s}$) and super high viscosity silicone oils ($\rho_{fluid} = 979 \text{ kg m}^{-3}$, $\mu = 293 \text{ Pa s}$). Fluids with custom viscosity can be created in principle by mixing various miscible fluids, e.g. water and glycerol or mineral and silicone oils. All silicone oil properties obtained from <http://www.clearcoproducts.com/>.

Particle (environmental fluid)	Size (L^0 , μm)	Particle density ($\rho_{particle}^0$, kg m^{-3})	Estimated Re^0	Estimated C_D^0	Working Fluid	Working fluid density (ρ_{fluid} , kg m^{-3})	Working fluid Viscosity (μ , Pa s)	Estimated Model Scale (S)	Estimated Model size (cm)	Estimated model U (cm s^{-1})	Species / reference
Foraminifera (water)	250 – 700	2830	3 - 40	1.5 – 10	Mineral oils	830	0.022	15	3.75	2 - 16	This study
Poppy seeds (air)	1500	1060	280	0.7	Medium viscosity silicone oils	960	0.048	37	6	25	<i>Papaver nudicaule</i> (Oskui et al., 2017)
Diatom skeletons (water)	250	2200	0.1	55	High viscosity silicone oils	975	4.875	560	14	8	<i>Melosira granulata</i> (Botte et al., 2013)
Radiolaria skeletons (water)	290	5500	0.2	440				870	25	0.4	means of 58 species (Takahashi & Honjo, 1983)
Fern Spores (air)	48	590	0.1	190				670	3	2	means of 23 species (Gómez-Noguez et al., 2016)